Open-State Disulfide Crosslinking between *Mycobacterium tuberculosis* Mechanosensitive Channel Subunits

George Shapovalov,*† Randal Bass,‡ Douglas C. Rees,‡§ and Henry A. Lester*
*Division of Biology; †Division of Physics, Mathematics, and Astronomy; ‡Division of Chemistry and Chemical Engineering; and §Howard Hughes Medical Institute; California Institute of Technology, Pasadena, California 91125

ABSTRACT The mechanosensitive channel of large conductance from *Mycobacterium tuberculosis* (Tb-MscL) was subjected to cysteine-scanning mutagenesis at several residues in the M1 region. The V15C channel displayed disulfide crosslinking in air, but not in the presence of 100 mM β-mercaptoethanol. In single-channel experiments, the V15C channel was more sensitive to tension than was wild-type Tb-MscL. In air, Tb-MscL V15C occasionally displayed signature-events: at constant tension, there was first a sojourn in the highest conductance open state, then a series of transitions to substates. During a signature-event, these transitions do not appear to be reversible. Some sojourns in the lower conductance states lasted for $\geq$100 s. These signature-events were abolished by 100 mM β-mercaptoethanol and did not occur in a cysteineless gain-of-function mutant, suggesting that the signature-events represent disulfide crosslinking between channel subunits. We conclude that the crosslinking occurs during an open state during asymmetric sojourns that bring the α-carbons of adjacent 15C side chains within 3.6–6.8 Å. Such asymmetric structures must be considered in models of TB-MscL gating.

INTRODUCTION

The mechanosensitive channel of large conductance from *Mycobacterium tuberculosis* (Tb-MscL) can be expressed in large quantities and is one of the few ion channels of known atomic-scale structure (Chang et al., 1998). Furthermore, MscL channels are amenable to the usual electrophysiological studies, suggesting the possibility of further research that combines biochemical, functional, and structural approaches.

Only the closed-state structure of Tb-MscL is presently known (Chang et al., 1998). To extend this knowledge, we have attempted to generate cysteine-containing mutants of TB-MscL that could potentially be trapped, by crosslinking, in other states (Sukharev et al., 2001a). In parallel electrophysiological experiments, we have noted distinct functional correlates of crosslinking. This paper reports these data.

Wild-type Tb-MscL does not gate readily under pressures attainable in experiments on normal membranes (Moe et al., 2000), rendering it less useful than originally hoped for electrophysiological characterization. Happily, recent experiments have generated several gain-of-function Tb-MscL mutants with increased sensitivity to membrane tension (Maurer and Dougherty, 2001; Maurer et al., 2000); and molecular dynamics calculations suggest other gain-of-function mutants (Elmore and Dougherty, 2001; Kong et al., 2002). One of the suggested mutations, Tb-MscL E104Q, has been generated and is employed in the present study as a cysteineless gain-of-function control channel. We now report that an informative Tb-MscL cysteine mutation also opens at attainable membrane tension; and we compare its functional characteristics to another gain-of-function mutant.

Submitted August 30, 2002, and accepted for publication December 9, 2002.

Address reprint requests to Henry A. Lester, Div. of Biology 156-29, California Institute of Technology, Pasadena, CA 91125. Tel.: 626-395-4946; Fax: 626-564-8709; E-mail: lester@caltech.edu.

© 2003 by the Biophysical Society

0006-3495/03/04/2357/09 $2.00

METHODS

Genetic manipulations

Mutations were constructed in the gene for wild-type Tb-MscL, as described (Chang et al., 1998). Mutants were engineered in MscL by PCR-based mutagenesis of the entire MscL gene. Mutants were subcloned into the T7 expression vector pet19B (Invitrogen) which placed a His_{10} tag at the N-terminus to aid in purification. These His_{10} tagged constructs were used for all biochemical and electrophysiological experiments. Plasmids bearing substituted MscL genes were transformed into an *Escherichia coli* strain deleted for wild-type MscL (MscL-KO, provided by C. Kung) with the addition of T7 RNA polymerase added chromosomally to allow for overexpression using the pet19b constructs. Transformants were grown overnight in LB + Ampicillin (100 μg/ml) shaken cultures and diluted 1:500 into 1L of Terrific Broth + Amp and grown until the OD_{600} reached ~1.0. Cultures were induced with 2% lactose and 2 mM IPTG for 2 h and harvested by centrifugation. Cells were extracted at 4°C in 20 mM Tris, pH 7.5, 150 mM NaCl, 10 mM EDTA, and 1% dodecylmaltoside (Anatrace) for 2–3 h. Solubilizations were clarified by centrifugation (20,000 × g for 30 min) and detergent-solubilized pentameric MscL channels were purified by Ni-NTA chromatography on an AKTA Explorer chromatography system (Amersham-Pharmacia Biotech) at 4°C.

Disulfide trapping

Detergent-solubilized and purified MscL protein, either the single-cysteine-containing mutant or wild type, was subjected to mild oxidation using Cu(II)-1,10-phenanthroline (1 mM) for 20–30 min at 37°C with quenching of unreacted thiols by *n*-ethylmaleimide. The resulting covalently crosslinked protein was visualized on 10% nonreducing Laemmli gels. Parallel reactions lacking the oxidant were also performed to assess levels of uncatalyzed disulfide formation. To determine the level of reductant necessary to fully reduce MscL after oxidation, a subset of reactions were reduced with varying concentrations of β-mercaptoethanol (βME) after oxidation and quenching with *n*-ethylmaleimide (5 mM).

Single-channel recording and analysis

Giant spheroplasts were prepared from the cells expressing TB-MscL V15C or E104Q mutants (provided by J. Maurer; also see Maurer and Dougherty, 2001) according to the procedures previously described (Blount et al., 1999; Martinac et al., 1987). Single-channel patch-clamp recordings were made with a bandwidth of 20 kHz at 90 mV (intracellular medium is negative) in symmetrical 200 mM KCl, 90 mM $MgCl_2$, 10 mM $CaCl_2$, 5 mM HEPES (pH 7.0). For the experiments investigating mutant gating in reducing conditions, recordings were made in the same buffer containing an additional 100 mM βME. Currents were acquired with an Axopatch 200B amplifier, digitized with a Digidata 1322A digitizer and recorded with pCLAMP 8 software. All recordings were done at room temperature.

In some cases, patches onto V15C membranes in normal buffer became unstable during the suction application to form seals, presumably due to a significant rate of spontaneous disulfide bond formation. Only the traces that contained clear single-channel activity after seal formation were taken for further analysis. Integration of single-channel currents in the traces was performed with the help of a locally written program, which was tested against manual analyses.

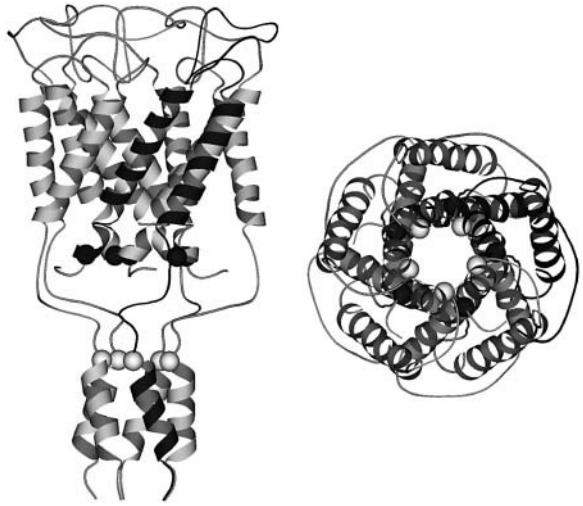

FIGURE 2 Crystal structure of the Tb-MscL protein showing a side view (*left*) and looking down the fivefold axis (*right*). One monomer of the homopentameric channel is highlighted. Light spheres denote the E104 position, whereas the dark spheres indicate the V15C position.

RESULTS

Disulfide scanning

A series of TB-MscL mutants were constructed with cysteines at all positions in transmembrane helices 1 and 2 (TM1 and TM2). To determine the optimal conditions for disulfide crosslinking of the MscL channels, we first purified MscL homopentameric channels via detergent extraction and nickel-affinity chromatography. The resulting detergent-solubilized protein was subjected to mild oxidation (1 mM Cu(II)-1,10-phenanthroline). For each position both unoxidized (monomer) and oxidized (covalent-dimer) samples were visualized on nonreducing polyacrylamide gels and stained by Coomassie (Fig. 1).

In the case of the wild-type protein, lacking cysteines, no change was detected in the mobility of the protein (data not shown). All cysteine mutants at positions along TM1 and TM2 (Fig. 2) displayed observable crosslinking. In general, positions in TM1 showed more complete crosslinking than those in TM2, perhaps as a result of the closer proximity of homologous positions. Positions at the N-terminus of TM1, including V15C and L17C, showed the greatest crosslinking (>50% under the conditions of Fig. 1).

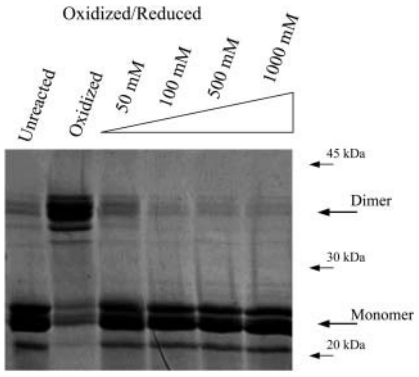

FIGURE 1 Oxidation/reduction of detergent-solubilized and purified Tb-MscL. (*Lanes* 1–6), unreacted protein, oxidized protein (1 mM $Cu(Phen)_3$), oxidized protein with subsequent addition of 50, 100, 500, and 1000 mM βME, respectively. Arrows denote the positions of the monomer and covalent dimer bands.

We conducted detailed studies of the V15C mutant. The V15C protein showed nearly complete oxidation during a 30-min reaction at 37°C, as revealed by the shift from monomer to dimer in Fig. 1. Because these engineered channels contain a single cysteine in each monomer, reaction with a homologous cysteine in another monomer presumably forms a covalent dimer, which is retained in the nonreducing SDS gel. Additional samples were oxidized identically and subsequently reduced with varying concentrations of βME to verify that the oxidation of the cysteines was fully reversible. At 50 mM reductant, some disulfide formation remains as revealed by the persistent dimer band. However, the addition of 100 mM βME appears sufficient to completely reduce the disulfides (Fig. 1).

Electrophysiological measurements

V15C and E104Q demonstrate a gain-of-function phenotype

This paper presents single-channel currents for V15C and E104Q Tb-MscL mutants expressed in a strain of *E. coli* that lacks native MscL channels. Both mutants appear to have a gain-of-function phenotype in comparison to the WT Tb-MscL channel. Fig. 3 presents dose-response (*suction*-P_{open}) relations for exemplar V15C (*solid rectangles*) and E104Q (*solid triangles*) channels, compared to the data for an *E. coli* MscS channel (*open circles*). We fitted a Boltzmann dis-

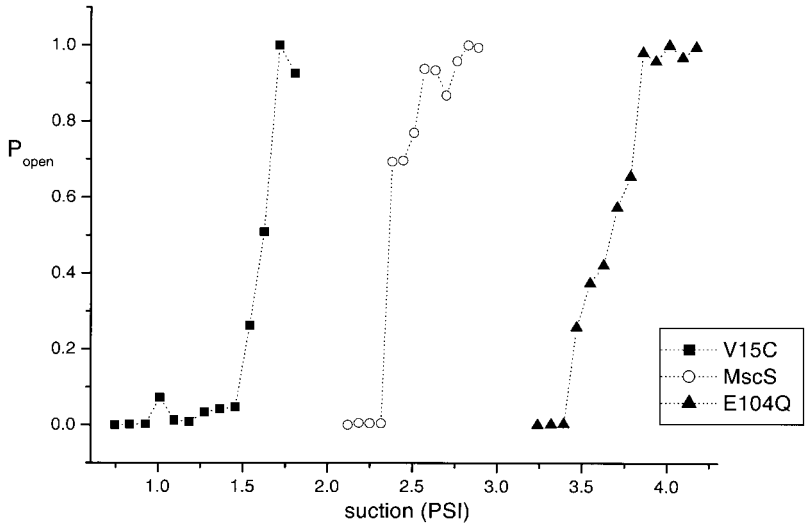

FIGURE 3 Representative dose-response (*suction-P_{open}*) relations for single V15C (*solid rectangles*) and E104Q (*solid triangles*) Tb MscL mutants and *E. coli* MscS (*open circles*) channels in spheroplasts prepared from *E. coli* MscL-deleted cells expressing these channels. Boltzmann distributions were fitted to the individual (P_{open}-*suction*) relations as shown on the figure. Midpoints were collected for every channel from at least four patches in each case and averaged. Midpoints and standard errors are 3.6 ± 0.3 PSI (25 ± 2 kPa) for E104Q, 1.6 ± 0.1 PSI (11 ± 1 kPa) for V15C, and 2.4 ± 0.1 PSI (17 ± 1 kPa) for *E. coli* MscS.

tribution to the dose-response relation constructed from each record. Midpoints (mean ± SE) are 3.6 ± 0.3 PSI (25 ± 2 kPa) for E104Q, 1.6 ± 0.1 PSI (11 ± 1 kPa) for V15C, and 2.4 ± 0.1 PSI (17 ± 1 kPa) for *E. coli* MscS. Thus the examples shown in Fig. 3 typify the relative mechanosensitivity, V15C > *E. coli* MscS > E104Q.

Mechanosensitive channels such as MscL and MscS are gated by membrane tension rather than directly by applied suction pressure. Therefore rigorous investigations of dose-response relations for the mutants often include normalization to the suction required to gate an internal control, such as *E. coli* MscS channels, in each patch. We rarely observed MscS activity at the level sufficient for such normalization in our patches, because of both the high expression levels of the Tb MscL mutants and (in the case of the V15C mutation) the severe gain-of-function phenotype. We avoided studying patches that did contain both MscL and MscS channels, primarily because the ''signature-events'' described in this article (below) involved many substates that could be confused with MscS gating events.

V15C shows atypical single-channel behavior: signature-events

We report that the V15C mutant exhibits an atypical electrophysiological activity: the presence of signature-events. These events are characterized in Fig. 4 through Fig. 9. Unlike during normal single-channel gating, signature-events display non-Markovian behavior. During such behavior, the channel enters a mode of persistent activity. The channel appears to open with no unusual steps and to the normal open level. However, the channel then undergoes a series of downward steplike transitions. The channel remains active even after the release of suction, undergoing frequent transitions among low-conductance substates.

Fig. 4 presents fragments of single-channel traces of E104Q (*A*) and V15C in normal buffer (*B*) and in buffer containing 100 mM βME (*C*). It can be seen that under regular physiological conditions V15C demonstrates a mixture of normal and atypical gating. The first few openings in the trace correspond to the normal single-channel activity; however, at t ~ 9 s, a signature-event occurs.

Signature-events were observed in traces of V15C activity in regular buffer on more than 25 occasions, from seven spheroplast preparations, on 11 days of recording. Roughly 60% of V15C traces contained signature-events. Signature-events appear to be non-Markovian: we have never observed a time-reversed signature-event, defined as a gradual progression, at constant suction, through substates of increasing conductance to the highest conductance state.

We first describe the macroscopic equivalent of signature-events; we then present more detailed analyses of the signature-events.

Persistent activity in macroscopic V15C traces

Because signature-events occur only once at individual channels and provide a high background conductance that vitiate further recording from a patch, it is tedious to study large numbers of signature-events. As an alternative approach to study these events, we sought and found evidence for signature-events in macroscopic traces of summed activity from many (6–20) V15C channels. Fig. 5 shows fragments of activity in macroscopic patches. E104Q (*A*) is compared to V15C in normal buffer (*B*) and with added 100 mM βME (*C*). All three traces show currents that activate in response to the applied suction. After the suction was released, the macroscopic currents of both the cysteineless mutant E104Q, as well as V15C under reducing conditions, returned to baseline. On the other hand, the V15C trace in normal buffer displays partial activity even after the suction was released.

These data provide the macroscopic equivalent of our single-channel measurements, as follows. The faster, reversible phase of macroscopic current is contributed by channels

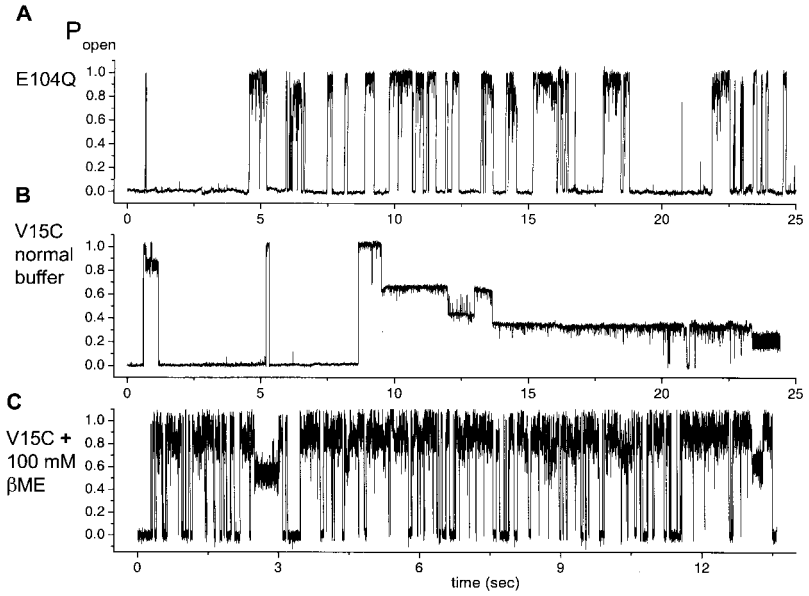

FIGURE 4 Comparison of single-channel activity of the cysteineless gain of function Tb-MscL mutant E104Q (*A*), V15C in a normal buffer (*B*), and V15C in a buffer containing 100 mM βME (*C*). E104Q in normal buffer and V15C in reducing buffer (*A* and *C*) demonstrate normal single-channel gating. *B* (V15C in normal buffer) demonstrates a non-Markovian behavior termed a signature-event. During such an event, the channel opens in a usual fashion; however, it then undergoes a series of steplike transitions to lower conductance. Activity is maintained even after suction is released.

that gate normally under the conditions of our experiments. This behavior is produced by control (cysteineless) channels or by V15C under reducing conditions. The sustained phase is produced by a subset of V15C channels that have undergone signature-events before or during the pressure pulse. Because the sustained conductance does not build up in the absence of pressure pulses, it is evident that activation of the channels produces a large increase (probably by several hundredfold) in the probability of a signature-event.

To provide a macroscopic kinetic characterization of this persistent-activity mode, we attempted two exponential fits to the macroscopic traces (data not shown). Time constants for the faster phases essentially equaled the time scale at which suction was released (0.3–1 s) and were comparable for all three test cases (for both mutants and for V15C under regular and reducing conditions). Thus, we could not identify a distinct molecular process during the faster phase. On the other hand, in traces with a sustained component that amounted to >20% of the total current, the slower phases typically were too long for systematic fitting; the time constant was at least 20 s. Thus the macroscopic traces provide a qualitative picture that complements the single-channel traces; but the macroscopic traces add little precise kinetic data.

Signature-events emphasize conductive substates of the channel

Thirteen well resolved signature-events were subjected to detailed analysis. Figs. 6 and 7 present a detailed view of a V15C channel signature-event on a time scale of a few

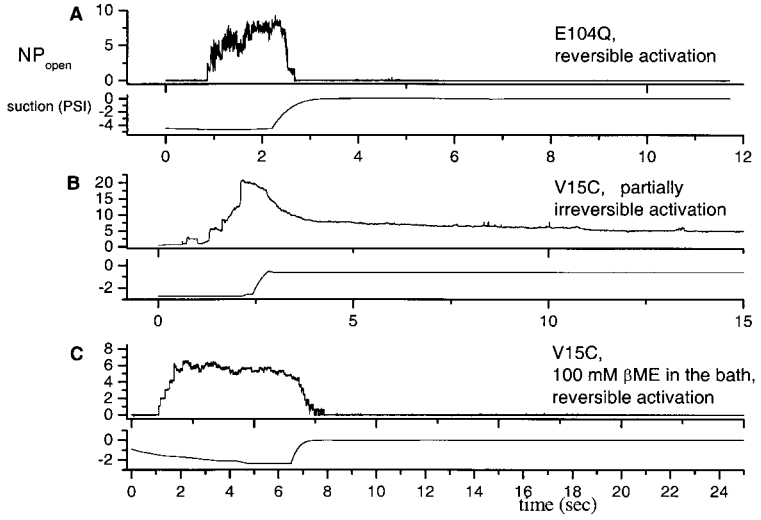

FIGURE 5 Comparison of activity in macroscopic patches: cysteineless gain of function Tb-MscL mutant E104Q (*A*), V15C in normal buffer (*B*), and V15C in a buffer containing 100 mM βME (*C*). Each panel displays current (*above*) and suction (*below*) traces. Macroscopic currents of E104Q in normal buffer and V15C in reducing buffer (*A* and *C*) return to the baseline after suction release. The trace for V15C in normal buffer (*B*) demonstrates a ''persistent tail'' representing maintained partial activity.

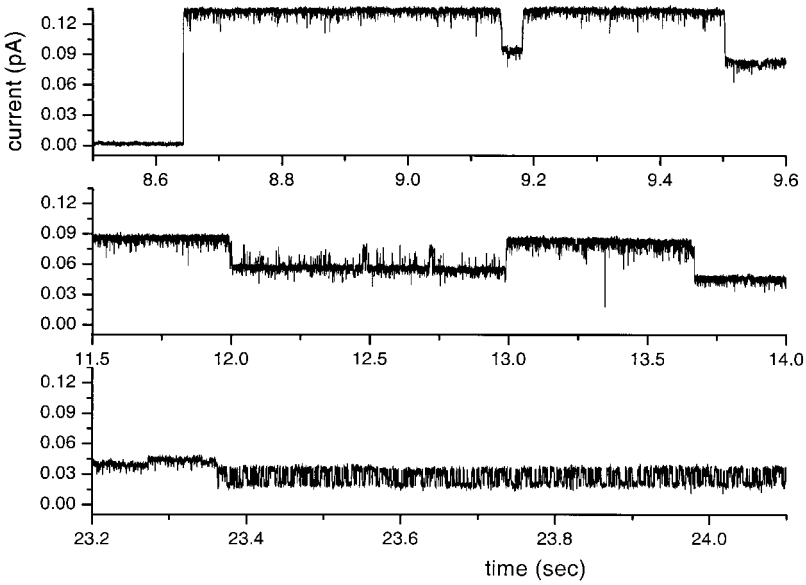

FIGURE 6 Details of a typical V15C signature-event. Traces show higher temporal resolution fragments (~1 s per panel) of the trace of V15C activity in normal solution presented in Fig. 4 *B*. The *x*-axis labels represent the corresponding time stamps of the parent trace.

seconds and a few hundred milliseconds, respectively. We emphasize the following common features of the 13 signature-events. At constant tension, there was first a sojourn in the highest conductance open state, then a series of transitions to substates. During a signature-event, these transitions do not appear to be reversible. Thus, the channel always enters the highest conductance state first and generally transitions through substates of decreasing conductance. The sojourn in the lower conductance states often lasted for tens and, in some cases hundreds, of seconds.

Fragments of V15C traces containing complete signature-events were analyzed to produce all-points histograms. These histograms were compared to similarly constructed histograms representing normal gating of the V15C mutant. Comparison of these histograms in Fig. 8 supports the empirical description that, during signature-events, the channel spends a significantly larger amount of time in conductance substates.

V15C loses apparent tension sensitivity during signature-events

In all 13 signature-events, the V15C channel lost its apparent mechanosensitivity. Fig. 9 demonstrates an exemplar trace: activity persisted in the lower conductive substates after suction has been reduced. Successive application of suction neither restored normal gating nor shifted the channel gating toward higher conductance substates.

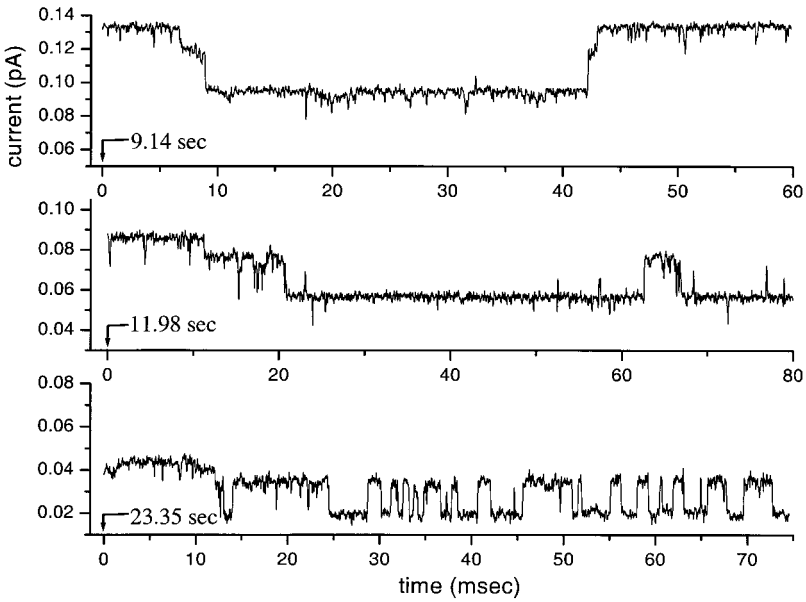

FIGURE 7 High temporal resolution fragments of the V15C trace presented in Fig. 4 *B*. Start times of each fragment provide a temporal alignment with the complete trace.

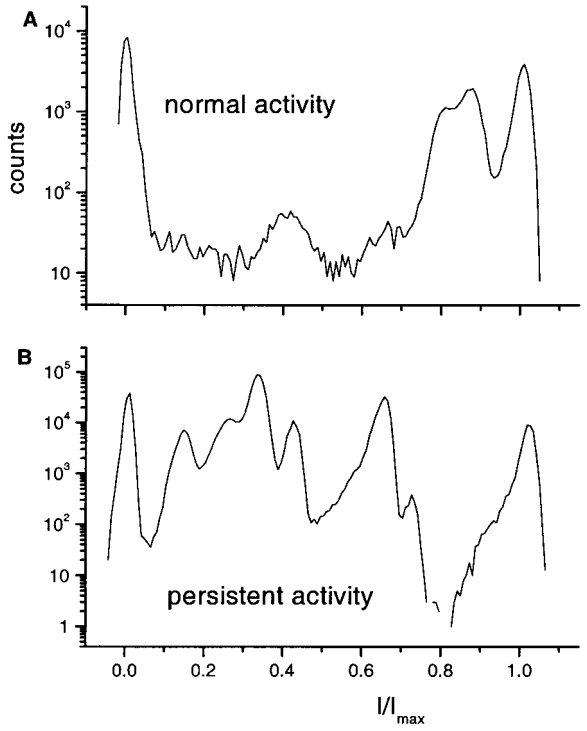

FIGURE 8 All-points histograms for a V15C mutant channel, during normal gating (*A*) and signature-events (*B*). The *y*-axis has a log scale to emphasize rare events. The channel spends a significant portion of time in conductive substates during signature-events. All-points histograms of normal V15C activity display minor peaks at intermediate conductances. However, no conclusion can be made about correspondence of substates during channel gating in normal and persistent modes.

The rate constant for crosslinking

To estimate a rate constant for the appearance of a signature-event, we analyzed long stretches of records from experiments with repeated suction pulses. We formulated three criteria to define V15C signature-events. The first two criteria describe characteristic features of atypical V15C gating. The last criterion allows us to filter out brief events:

1. Non-Markovian gating. After a sojourn in the highest conductance state, the channel performs a series of downward transitions. There are frequent transitions between neighboring substates (ruling out a leaky membrane). Conductance gradually shifts toward lower substates.
2. Loss of apparent tension sensitivity. The channel maintains activity even after suction has been reduced.
3. Persistent activity. Activity characterized by the above two criteria must persist for $\geq$10 s.

These criteria were applied during the analysis of the patches of V15C and E104Q either in normal buffer or with 100 mM added βME (13 and five patches, respectively, for V15C and six and five for E104Q). At least 120 s of activity were recorded for each patch. Pressure pulses of 10-s duration were applied at 20-s intervals to test for pressure independence.

We converted traces to lists of NP_{open} versus time, by dividing (deviations from the baseline)/(single-channel current). We then integrated these lists over time to form a value T, the cumulative open time for all channels in the patch, with dimensions $NP_{open} \times$ s. We counted the total number of signature-events, S, during these episodes. The ratio S/T gives a first-order rate constant, termed k_s in Table 1 and in Fig. 10 (described below), for the transition from the open state of the channel to a crosslinked state. The parameter k_s is almost certainly a composite rate constant (see Discussion). The value of k_s is 0.04 s^{-1} for V15C in normal buffer (Table 1).

Certain idiosyncrasies limit the precision of this analysis. Some finite-conductance ''tails'' of signature-events persisted until the start of the next episode, artifactually

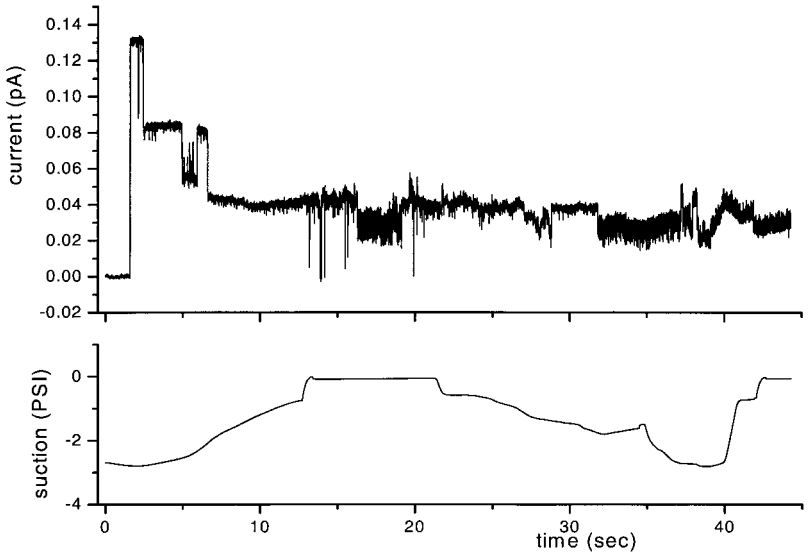

FIGURE 9 Recording of a signature-event (*upper trace*) while the patch was subject to variable suction (*lower trace*). Note that once the event has begun, changes in suction neither close the channel nor shift gating toward the states of higher conductance.

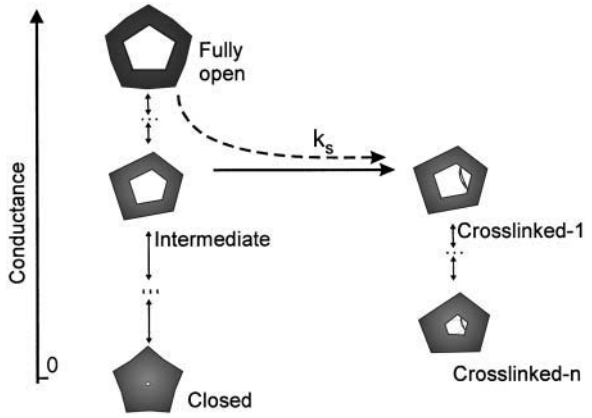

FIGURE 10 Cartoon presenting possible molecular events during a signature-event. Intermediate states are ordered according to conductance, which increases along the vertical axis; no specific kinetic model is implied. Transitions in the horizontal direction represent S-S bond formation. The text explains the geometric reasoning for the suggestion that cysteine crosslinking occurs from an asymmetric intermediate state rather than from the fully open state of the channel. Asymmetry is implied by the fact that two of the walls are shorter than the other three. The dashed single-headed arrow (k_s) from the fully open state to the crosslinked-1 state represents a composite rate constant, comprising sojourns in one or more intermediate states. After crosslinking occurs, activity of the channel is dominated by the newly formed bond. This is represented in a cartoon by asymmetric drawings of crosslinked states.

increasing the cumulative open time T in the traces that contained such events. To minimize this offset we ignored intersweep intervals that contained only persistent tails of signature-events and corrected the baseline where appropriate. We estimate that the errors introduced by the persistent tails are $\leq$10%.

The rate constant for crosslinking is essentially zero for V15C in 100 mM βME and for E104Q

The signature-events appear under conditions that correspond to the disulfide crosslinking observed biochemically (Fig. 1). To test the hypothesis that signature-events result from crosslinking, we compared records from V15C under control conditions versus reducing conditions that prevented crosslinking in the biochemical experiments (Fig. 1). In the case of V15C in 100 mM βME, no definitive signature-events were observed. Thus the value presented in Table 1 defines a ''less than'' estimate of the rate constant k_s for the transition from the open state to a crosslinked state of V15C channels under reducing conditions. This rate constant is thus less than one tenth of the value under normal conditions. The data of Table 1 support the biochemical observation of noticeable self-oxidation of V15C in normal buffer (Fig. 1).

TABLE 1 Analysis of the rate constant, k_s, for transitions from the fully open state to signature-events

	No. sweeps	Rate constant for transition to signature-event, k_s (s^{-1})
Normal buffer	13	0.04
100 mM βME	12	$<3.1 \times 10^{-3}$

The number of analyzed suction sweeps and k_s are given for V15C channel in regular buffer and with added 100 mM βME. The ''less than'' sign in the second row indicates that we observed no definitive signature-events in the V15C traces when reducing agent was added to the buffer. Thus the reported value serves only as a ''less than'' estimate.

Traces of E104Q activity contained a small number of events satisfying criterion (*1*), a steplike conductance reduction. However these events were suction-dependent and thus did not satisfy the definition of signature-event criteria.

An additional observation supports the view of a signature-event as an oxidative crosslinking. A relatively low proportion (~25%) of traces of V15C activity in normal buffer yielded data suitable for analysis, primarily because after a signature-event, many patches became unstable and thus were excluded from the analysis. A higher proportion (~65%) of control traces (V15C in 100 mM βME and both conditions for E104Q) yielded relatively stable patches that could sustain multiple suction pulses. Taken together with the above results, these anecdotal observations support the hypothesis that spontaneous disulfide bonds form in V15C.

L17C shows no signature-events

We performed similar experiments on the L17C mutant. We found no signature-events under either oxidizing or reducing conditions. Analysis of these data shows that the rate constant k_s is less than 3×10^{-3} s, which also corresponds to the upper limit for V15C under reducing conditions. Thus, signature-events are not a general property of Tb-MscL cysteine mutant channels.

DISCUSSION

The data clearly indicate that the TB-MscL V15C channel can undergo an oxidative intersubunit disulfide crosslinking event. Although previous studies show that disulfide crosslinks can occur between two cysteine residues at different positions within a subunit or across subunits, the present study concerns crosslinks between cysteines at identical positions in two subunits (Betanzos et al., 2002; Sukharev, 2002). Such a crosslinking event can occur only if the α-carbon atoms of adjacent 15C residues approach each other within 3.6–6.8 Å (Falke et al., 1988; Pantoliano et al., 1987; Perry and Wetzel, 1986; Srinivasan et al., 1990). The crystal structure of the Tb-MscL channel in the closed state (Chang et al.) reveals that the α- and β-carbon atoms of V15 residues on neighboring subunits are 10.5 and 12.0 Å apart, respectively; and molecular dynamics simulations (Elmore and Dougherty, 2001) reveal that the α-carbon atoms of V15 residues do not approach each other closer than 10 Å on the ~1-ns time scale of such simulations (D. Elmore, personal communication). These arguments imply that the two side

chains approach each other during another state. What is this crosslinkable state, and what are the implications for the structure of Tb-MscL in states that have not yet been crystallized?

The crosslinking presumably occurs soon after the start of a signature-event. Most conceptual models of MscL channel opening involve dilation of the pore; and in all such models, a symmetrical dilation would imply that all subunits increase rather than decrease their distance. Specifically the distance between equivalent residues on adjacent subunits cannot be smaller than $D \times \sin(\pi/5)$, where D is the pore diameter. This value, known at 10.5–12 Å for the closed state (see above), can be calculated at 18 Å for the pore diameter of 30 Å as reported for MscL channels (Blount et al., 1999; Cruickshank et al., 1997), and is presumably an intermediate value for symmetric states of intermediate conductance. Therefore a symmetrical dilation associated with *any* state of the channel—closed, intermediate, or fully open—would decrease, rather than increase, the likelihood of a crosslinking event. We are led to the conclusion that crosslinking occurs during a rare asymmetric local motion of the channel protein in which the 15C residues of two adjacent M1 helices approach each other (Fig. 10). In brief, we conclude that the presence of crosslinking between the 15C residues of adjacent MscL subunits reveals the presence of transient, presumably local, and probably asymmetric conformations allowing close approach of two subunits. One likely hypothesis is that the asymmetric local event is a corkscrew motion of an M1-helix in a single subunit (Perozo et al., 2002; Sukharev et al., 2001a; Yoshimura et al., 1999). Previous data also show that disulfide bonds occasionally form between cysteine residues that are distant in crystal structures (Butler and Falke, 1996).

Asymmetric conformations of intermediate conductive states of *E. coli* MscL channel have been postulated previously (Sukharev et al., 2001a,b). However the previously proposed asymmetry involves rearrangement of the N-terminal domains only (these are not resolved in the Tb MscL crystal structure), leaving the M1 helices in a symmetric conformation.

Our ideas about the crosslinking are presented in the cartoon of Fig. 10. The crosslinking occurs during an opening, and in particular during a sojourn at a subconductance state. This suggestion is based on the fact that the opening transition to a signature-event is unremarkable (at least on our time scale), that the fully open state is the last ''normal'' state in a trace that then becomes abnormal, and that this highest conductance state presumably has radial symmetry, the largest diameter, and therefore the greatest distance between 15C residues, and therefore would disfavor the transient local approach that we postulate. The local approach of two adjacent 15C residues would be trapped by the formation of a disulfide bond. The closed state presumably represents the closest approach of the 15C residues that occurs in a symmetrical structure, but the crosslinking occurs while the channel is at least partially open, and therefore we conclude that the crosslinkable state is an asymmetric one. Although the cartoon of Fig. 10 is drawn, for simplicity, as though the crosslinkable state is a necessary intermediate state during the normal gating of channel, the crosslinkable state may actually be on a side pathway. We cannot yet guess whether the transient, crosslinkable state lasts picoseconds, nanoseconds, or microseconds; but there is ample evidence that the channel visits substates during normal activity (for instance, Fig. 8). The parameter k_s denotes the rate of such a transition from the open state, and is reported in the Table 1 at 0.04 s^{-1} for normal buffer and at $< 3.1 \times 10^{-3}$ s^{-1} under reducing conditions. Our value of k_s agrees well with the rate constant of 0.3 s^{-1} for formation of disulfide bonds between two cysteine side chains introduced into the pore of a Na^+ channel (Benitah et al., 1996) and lies within the range for optimally aligned cysteine residues that can form disulfide bonds with minimal translational motion (Careaga and Falke, 1992).

In any case, once the crosslinking occurs, the channel eventually becomes most likely to occupy states of fractional conductance, which typify the trace after 10–20 s in most of the signature-events. The channel's state is now apparently dominated by the covalent crosslink rather than by externally applied tension. In rough agreement with these conclusions, a previous report shows that the *E. coli* I3C, F7C, and F10C channels also become crosslinked and can open only to subconductance states (Sukharev et al., 2001a). However, the previous report did not reveal whether the crosslinking is associated with a transient opening to the fully open state, as we have observed. If our observation is a general one, then dynamic models of Tb-MscL structure need to account for local asymmetric movements; and existing symmetric structural models (Sukharev et al., 2001b) should be interpreted as time-averaged pictures that might comprise a range of asymmetric intermediate states.

We thank Sergei Sukharev and Paul Blount for introducing us to MscL electrophysiology, Josh Maurer for mutants and cells, and Ido Braslavsky, Donald Elmore, Steve Quake, Gerd Kochendoerfer, and Dennis Dougherty for valuable discussion.

This research was supported by a grant from the National Institutes of Health (GM-062532), by a Burroughs-Wellcome Fund Computation and Molecular Biology Fellowship to George Shapovalov, and by an National Research Service Award to Randal Bass (GM-020705).

REFERENCES

Benitah, J. P., G. F. Tomaselli, and E. Marban. 1996. Adjacent pore-lining residues within sodium channels identified by paired cysteine mutagenesis. *Proc. Natl. Acad. Sci. USA*. 93:7392–7396.

Betanzos, M., C. S. Chiang, H. R. Guy, and S. Sukharev. 2002. A large iris-like expansion of a mechanosensitive channel protein induced by membrane tension. *Nat. Struct. Biol.* 9:704–710.

Blount, P., S. I. Sukharev, P. C. Moe, B. Martinac, and C. Kung. 1999. Mechanosensitive channels of bacteria. *Methods Enzymol.* 294:458–482.

Butler, S. L., and J. J. Falke. 1996. Effects of protein stabilizing agents on thermal backbone motions: a disulfide trapping study. *Biochemistry*. 35:10595–10600.

Careaga, C. L., and J. J. Falke. 1992. Thermal motions of surface α-helices in the D-galactose chemosensory receptor. Detection by disulfide trapping. *J. Mol. Biol.* 226:1219–1235.

Chang, G., R. H. Spencer, A. T. Lee, M. T. Barclay, and D. C. Rees. 1998. Structure of the MscL homolog from *Mycobacterium tuberculosis*: a gated mechanosensitive ion channel. *Science*. 282:2220–2226.

Cruickshank, C. C., R. F. Minchin, A. C. Le Dain, and B. Martinac. 1997. Estimation of the pore size of the large-conductance mechanosensitive ion channel of *Escherichia coli*. *Biophys. J.* 73:1925–1931.

Elmore, D. E., and D. A. Dougherty. 2001. Molecular dynamics simulations of wild-type and mutant forms of the *Mycobacterium tuberculosis* MscL channel. *Biophys. J.* 81:1345–1359.

Falke, J. J., A. F. Dernburg, D. A. Sternberg, N. Zalkin, D. L. Milligan, and D. E. Koshland, Jr. 1988. Structure of a bacterial sensory receptor. A site-directed sulfhydryl study. *J. Biol. Chem.* 263:14850–14858.

Kong, Y., Y. Shen, T. E. Warth, and J. Ma. 2002. Conformational pathways in the gating of *Escherichia coli* mechanosensitive channel. *Proc. Natl. Acad. Sci. USA*. 99:5999–6004.

Martinac, B., M. Buechner, A. H. Delcour, J. Adler, and C. Kung. 1987. Pressure-sensitive ion channel in *Escherichia coli*. *Proc. Natl. Acad. Sci. USA*. 84:2297–2301.

Maurer, J. A., and D. A. Dougherty. 2001. A high-throughput screen for MscL channel activity and mutational phenotyping. *Biochim. Biophys. Acta*. 1514:165–169.

Maurer, J. A., D. E. Elmore, H. A. Lester, and D. A. Dougherty. 2000. Comparing and contrasting *Escherichia coli* and *Mycobacterium tuberculosis* mechanosensitive channels (MscL). New gain of function mutations in the loop region. *J. Biol. Chem.* 275:22238–22244.

Moe, P. C., G. Levin, and P. Blount. 2000. Correlating a protein structure with function of a bacterial mechanosensitive channel. *J. Biol. Chem.* 275:31121–31127.

Pantoliano, M. W., R. C. Ladner, P. N. Bryan, M. L. Rollence, J. F. Wood, and T. L. Poulos. 1987. Protein engineering of subtilisin BPN′: enhanced stabilization through the introduction of two cysteines to form a disulfide bond. *Biochemistry*. 26:2077–2082.

Perozo, E., D. M. Cortes, P. Sompornpisut, A. Kloda, and B. Martinac. 2002. Open channel structure of MscL and the gating mechanism of mechanosensitive channels. *Nature*. 418:942–948.

Perry, L. J., and R. Wetzel. 1986. Unpaired cysteine-54 interferes with the ability of an engineered disulfide to stabilize T4 lysozyme. *Biochemistry*. 25:733–739.

Srinivasan, N., R. Sowdhamini, C. Ramakrishnan, and P. Balaram. 1990. Conformations of disulfide bridges in proteins. *Int. J. Pept. Protein Res.* 36:147–155.

Sukharev, S. 2002. Purification of the small mechanosensitive channel of *Escherichia coli* (mscs): the subunit structure, conduction, and gating characteristics in liposomes. *Biophys. J.* 83:290–298.

Sukharev, S., M. Betanzos, C. S. Chiang, and H. R. Guy. 2001a. The gating mechanism of the large mechanosensitive channel MscL. *Nature*. 409:720–724.

Sukharev, S., S. R. Durell, and H. R. Guy. 2001b. Structural models of the MscL gating mechanism. *Biophys. J.* 81:917–936.

Yoshimura, K., A. Batiza, M. Schroeder, P. Blount, and C. Kung. 1999. Hydrophilicity of a single residue within MscL correlates with increased channel mechanosensitivity. *Biophys. J.* 77:1960–1972.